Effects of interference in the dynamics of spin-1/2 transverse XY Chain driven periodically through quantum critical points

Victor Mukherjee[1,*] and Amit Dutta[1,†]

[1]Department of Physics, Indian Institute of Technology, Kanpur 208 016, India

(Dated: May 25, 2009)

We study the effects of interference on the quenching dynamics of a one-dimensional spin 1/2 XY model in the presence of a transverse field ($h(t)$) which varies sinusoidally with time as $h = h_0 \cos \omega t$, with $|t| \leq t_f = \pi/\omega$. We have explicitly shown that the finite values of t_f make the dynamics inherently dependent on the phases of probability amplitudes, which had been hitherto unseen in all cases of linear quenching with large initial and final times. In contrast, we also consider the situation where the magnetic field consists of an oscillatory as well as a linearly varying component, i.e., $h(t) = h_0 \cos \omega t + t/\tau$, where the interference effects lose importance in the limit of large τ. Our purpose is to estimate the defect density and the local entropy density in the final state if the system is initially prepared in its ground state. For a single crossing through the quantum critical point with $h = h_0 \cos \omega t$, the density of defects in the final state is calculated by mapping the dynamics to an equivalent Landau Zener problem by linearizing near the crossing point, and is found to vary as $\sqrt{\omega}$ in the limit of small ω. On the other hand, the local entropy density is found to attain a maximum as a function of ω near a characteristic scale ω_0. Extending to the situation of multiple crossings, we show that the role of finite initial and final times of quenching are manifested non-trivially in the interference effects of certain resonance modes which solely contribute to the production of defects. Kink density as well as the diagonal entropy density show oscillatory dependence on the number of full cycles of oscillation. Finally, the inclusion of a linear term in the transverse field on top of the oscillatory compo nent, results to a kink density which decreases continuously with τ while increases monotonically with ω. The entropy density also shows monotonous change with the parameters, increasing with τ and decreasing with ω, in sharp contrast to the situations studied earlier. We do also propose appropriate scaling relations for the defect density in above situations and compare the results with the numerical results obtained by integrating the Schrödinger equations.

PACS numbers:

I. INTRODUCTION

The phenomena of quantum phase transitions occurring at absolute zero temperature have attracted serious attention of scientists in recent years[1,2]. A quantum critical point is associated with a diverging length scale (ξ) and a diverging time scale (ξ_τ) which satisfy the scaling forms $\xi \sim |\overline{d}|^{-\nu}$ and $\xi_\tau \sim \xi^z$ in the vicinity of the quantum critical point. Here $\overline{d}$ denotes the deviation from the critical point, and ν, z are the corresponding critical exponents. Following the possibility of experimental studies of quantum systems trapped in optical lattices[3], there is a recent interest in theoretical studies of the related models[4,5]. When a parameter of the Hamiltonian of the system is swept across a quantum critical point. The diverging relaxation time near the quantum critical point forces the system to undergo non-adiabatic evolution irrespective of the rate of change of parameters. If the system is in its ground state at initial time, non-adiabatic transitions are manifested in the occurrence of non-zero 'defects' (called kinks) and non-zero local entropy in the system.

According to the Kibble-Zurek argument, if a parameter of the Hamiltonian is varied as t/τ, the density of defects (n) in the final state is expected to scale as $n \sim \tau^{-\nu d/(\nu z+1)}$, where d is the spatial dimensionality of the system[6,7,8,9].The above scaling form has been verified for quantum spin systems quenched through critical points[10,11,12,13] and also generalized to the cases of non-linear quenching[14] when a parameter is quenched as $h(t) \sim |t/\tau|^{|a|} sgn(t)$, for gapless systems[15] and also for quantum systems with disorder[16] and systems coupled to external environment[17]. Recently, a generalized form of the Kibble-Zurek scaling has been introduced which includes a situation where the system is quenched through the multicritical point[18] which shows that the general expression for kink density can be given as $n \sim \tau^{-d/2z_2}$, where z_2 determines the scaling of the off-diagonal term of the equivalent Landau-Zener problem close to the critical point.

In parallel to the studies on spin chains in condensed matter physics, great progress has also been made in the realm of quantum optics in exploring the dynamics of two level systems undergoing landau Zener tunneling due to oscillatory temporal variation of the parameters[19,20,21,22]. The Landau Zener transition probabilities have been calculated for single crossing as well as for multiple crossings. Superposition of a linear field along with the sinusoidally varying energy levels gives rise to an altogether different situation, which has also been studied thoroughly in recent years[23].

In our present work we exploit the techniques used in the above papers to explore the dynamics of one dimensional spin 1/2 chain undergoing quantum phase transitions due to the application of an oscillatory or an oscillatory as well as a linearly varying magnetic field and com-

pare the results with the earlier findings. Investigation of the dynamics of one dimensional transverse XY model under repeated quenching of linearly varying transverse magnetic field has been carried out in a recent work[24] and was shown that the defect density decreases in the reverse path though the entropy density increases monotonically with the number of quenching. However, the scaling of the defect density and the local entropy density when the quantum critical point is crossed due to a sinusoidal variation of the magnetic field has not been attempted before. Sinusoidal quenching puts an upper bound to the initial and final times, which makes the process of coarse graining invalid in the present scenario. The resultant dynamics of the system becomes dependent on the phases of the probability amplitudes, leading to the occurance of constructive or destructive interferences. The spin-1/2 transverse XY chain[25] discussed in this paper is described by the Hamiltonian

$$H = -\frac{1}{2}\sum_n (J_x\sigma_n^x\sigma_{n+1}^x + J_y\sigma_n^y\sigma_{n+1}^y + h\sigma_n^z), \qquad (1)$$

where the σ's are Pauli spin matrices satisfying the usual commutation relations and the interactions and the transverse field are denoted by J_x, J_y and h, respectively, with J_x, J_y and h all non-random. The interaction strength J_x and J_y are always time-independent whereas we shall use time-dependent transverse field in the subsequent sections.

The Hamiltonian in Eq. (1) can be exactly diagonalized using the Jordan-Wigner (JW) transformation which maps a system of spin-1/2's to a system of spinless fermions[25,26] given by

$$c_n = \exp\left(i\pi\sum_{j=1}^{n-1}\sigma_j^z\right)\sigma_n^-, \qquad (2)$$

where $\sigma_n^\pm = (\sigma_n^x \pm i\sigma_n^y)/2$ and the operator $\sigma_n^z = 2c_n^\dagger c_n - 1$ and the operators c_n satisfy the fermionic anti-commutation relations. In terms of JW fermions, the above Hamiltonian can be rewritten in Fourier space with a periodic boundary condition as

$$H = -\sum_{k\rangle 0}\{\ [(J_x+J_y)\cos k + h]\ (c_k^\dagger c_k + c_{-k}^\dagger c_{-k}) + i(J_x-J_y)\sin k\ (c_k^\dagger c_{-k}^\dagger + c_k c_{-k})\}. \qquad (3)$$

Diagonalizing the Hamiltonian in terms of the Bogoliubov fermions, we arrive at an expression for the gap in the excitation spectrum given by[25,26]

$$\epsilon_k = [h^2 + J_x^2 + J_y^2 + 2h(J_x+J_y)\cos k + 2J_xJ_y\cos 2k]^{1/2}. \qquad (4)$$

The gap given in Eq. (4) vanishes at $h = \mp(J_x+J_y)$ for wave vectors $k = 0$ and π respectively, signaling a quantum phase transition from a ferromagnetically ordered phase to a quantum paramagnetic phase known as the "Ising" transition[26]. On the other hand, the vanishing of gap at $J_x = J_y$ for $|h| < (J_x+J_y)$ at an ordering wavevector $k_0 = \cos^{-1}(-h/2J_x)$ signifies a quantum phase transition, belonging to a different universality class from the Ising transitions, between two ferro-magnetically ordered phases.

The advantage of employing the JW transformation is that when projected to the two-dimensional subspace spanned by $|0\rangle$ and $|k,-k\rangle$, the Hamiltonian takes the form $H = \sum_k H_k$ where the reduced Hamiltonian is written in the form

$$H_k(t) = -[h + (J_x+J_y)\cos k]\ I_2 + \begin{bmatrix} h+(J_x+J_y)\cos k & i(J_x-J_y)\sin k \\ -i(J_x-J_y)\sin k & -h-(J_x+J_y)\cos k \end{bmatrix},$$

where I_2 denotes the 2×2 identity matrix. Therefore, the many-body problem is effectively reduced to the problem of a two-level system with two levels denoted by the states $|0\rangle$ and $|k,-k\rangle$ which we refer to as diabatic basis vectors. We shall denote the basis vectors as $|0\rangle$ and $|k,-k\rangle$ as $|1\rangle$ and $|2\rangle$, respectively in this work for notational convenience and refer the states as diabatic energy levels.

The paper is organized in the following way: We have already discussed the model we are going to study. In section II, we discuss the case of oscillatory magnetic field but restrict our attention to the situation when the quantum critical points are crossed only once while in section III the possibility of multiple crossing is included. Section IV is used to discuss the dynamics with a magnetic field which has both linearly varying and oscillatory components. In every situation results obtained through approximate analytical methods are contrasted with the numerical ones obtained by direct integration. Conclusion and summary of the results are presented in the last section.

II. OSCILLATORY QUENCHING THROUGH A QUANTUM CRITICAL POINT: SINGLE CROSSING

In this section, we shall study the spin chain driven by an oscillatory transverse field given by $h(t) = h_0\cos\omega t$ from an initial time $-\pi/\omega$ to a final time 0 so that it crosses the gapless point only once during the course of evolution. The system initially prepared in the ground state $|1\rangle$ whereas the final ground state is $|2\rangle$. We shall evaluate the probability of the state $|1\rangle$ in the final state due to non-adiabatic evolution through the gapless point. As discussed above, the transverse XY chain Hamiltonian can be written as direct sum of 2×2 reduced Hamiltonian matrices H_k. For an oscillatory transverse field, the reduced Hamiltonian gets modified to

$$H_k(t) = \begin{bmatrix} h_0\cos\omega t + (J_x+J_y)\cos k & i(J_x-J_y)\sin k \\ -i(J_x-J_y)\sin k & -h_0\cos\omega t - (J_x+J_y)\cos k \end{bmatrix},$$

For any given mode k, the instantaneous energy gap of the Hamiltonian is minimum at a time $t_{0,k}$ such that

$h_0 \cos\omega t_{0,k} + (J_x + J_y)\cos k = 0$ where the diabatic levels cross each other. On the other hand, the energy gap vanishes for the wavevectors $k = 0$ and $k = \pi$ at a time $\cos\omega t = \mp(J_x + J_y)\cos k/h_0$, respectively, signalling the quantum phase transition of Ising class.

Denoting the probability amplitudes for the states $|1\rangle$ and $|2\rangle$ as $\overline{C_{1,k}}(t), \overline{C_{2,k}}(t)$, respectively, a general state vector in the reduced Hilbert space is witten as.

$$\psi_k(t) = \overline{C_{1,k}}(t)|1\rangle + \overline{C_{2,k}}(t)|2\rangle \tag{5}$$

Henceforth, we set $(J_x + J_y) = J$, and modulus of the off-diagonal terms $= |J_x - J_y|\sin k$ is denoted by Δ_k. Also the modulus of rate of change of the diagonal terms at time $t = t_{0,k}$ (given by $h_0\omega\sin\omega t_{0,k}$) is denoted bt α_k. Using the transformations

$$\begin{aligned}
\overline{C_{1,k}}(t) &= C_{1,k}(t)e^{-i\int^t dt'[h_0\cos\omega t + J\cos k]} \\
\overline{C_{2,k}}(t) &= C_{2,k}(t)e^{-i\int^t dt'[-h_0\cos\omega t - J\cos k]}
\end{aligned} \tag{6}$$

we can rewrite the Schrödinger equation describing the time evolution of the probability amplitudes in the form

$$\begin{aligned}
i\frac{dC_{1,k}(t)}{dt} &= \Delta_k C_{2,k}(t)e^{2i\int^t dt'[h_0\cos\omega t + J\cos k]} \\
i\frac{dC_{2,k}(t)}{dt} &= \Delta_k C_{1,k}(t)e^{-2i\int^t dt'[h_0\cos\omega t + \cos k]}.
\end{aligned} \tag{7}$$

It should be noted that for large values of $[h_0\cos\omega t + J\cos k]$, the phase factors on the r.h.s. of eq. (7) oscillate rapidly in time. As a result the amplitudes $C_{1,k}(t)$, $C_{2,k}(t)$, averaged over small intervals of time, remain basically constant in time. On the other hand, close to $t = t_{0k}$, the phase factors assume stationary values, thus leading to non-adiabatic transition between the energy levels[22,27,28].

In this section, we prepare the system in the ground state with initial conditions at $\omega t = -\pi$, i.e., $C_{1,k}(-\pi) = 1$ and $C_{2,k}(-\pi) = 0$ and the state evolves to $t = 0$ so that the spin chain crosses the gapless quantum critical point only once. Using Eqs. (7), one can arrive at the differential equation describing the amplitude $C_{1,k}(t)$ given by

$$\frac{d^2C_{1,k}}{d^2t} - 2i(h_0\cos\omega t + J\cos k)\frac{dC_{1,k}}{dt} + \Delta_k^2 C_{1,k} = 0 \tag{8}$$

with the probability of defect in the final state at $t = 0$ given by $p_k = |C_{1,k}(0)|^2$. The maximum contribution to the non-adiabatic transition probability comes from near the points where the energy gap between the instantaneous levels is minimum. We can therefore linearize the term $h_0\cos\omega t$ in the neighbourhood of $t_{0,k}$ to get

$$\frac{d^2C_{1,k}}{d^2t} - 2i(-h_0\omega(t - t_{0,k})\sin\omega t_{0,k})\frac{dC_{1,k}}{dt} + \Delta_k^2 C_{1,k} = 0 \tag{9}$$

Eq. (9) resembles the standard Landau Zener transition problem[28] for the linear quenching of the magnetic field with a variation of the field $h = t/\tau_{\rm eff}$ where $\tau_{\rm eff}$ is given by the the rate of change of the diagonal terms of the Hamiltonian (1). Therefore, let us define $\alpha_k = 1/\tau_{\rm eff} = \frac{d}{dt}(\epsilon_1 - \epsilon_2)|_{t_{0,k}} = 2h_0\omega\sin\omega t_{0,k} = 2\omega\sqrt{h_0^2 - J^2\cos^2 k}$. The non-adiabatic excitation probability[28] is given as $p_k = |C_{1,k}(0)|^2 = e^{-2\pi\gamma_k}$, where $\gamma_k = \Delta_k^2/|\frac{d}{dt}(\epsilon_1 - \epsilon_2)|_{t_{0,k}}$, leading to

$$p_k = e^{-\frac{\pi\Delta_k^2}{\omega\sqrt{h_0^2 - J^2\cos^2 k}}} \tag{10}$$

At this point, the natural question to ask is that for what values of the parameter h_0 and ω, the above relation of p_k is applicable. Of course, we have used the non-adiabatic transition probability of the standard linear Landau Zener problem where time t evolves from $-\infty$ to $+\infty$. The linearization near the crossing point employed above holds good only for small ω. More precisely, as discussed below the linearization approximation is applicable when the the time period of one cycle of the magnetic field $(2\pi/\omega)$ is much greater than the Landau Zener transition time $(T_{LZ,k})$ for a single crossing. The dimensionless Landau-Zener transition time[29,30] is defined as $\kappa_{LZ,k} = \sqrt{\alpha_k}T_{LZ,k} = |C_{2,k}(\overline{t})|^2/\frac{d}{d\kappa}|C_{2,k}(0)|^2 \approx |C_{2,k}(+\infty)|^2/(\frac{d}{d\kappa}|C_{2,k}(0)|^2)$, where $\kappa = \sqrt{\alpha_k}t$. Using the above definition, we find that $T_{LZ,k} \sim \Delta_k/\alpha_k$ in the adiabatic limit $(\Delta_k^2/\alpha_k >> 1)$ whereas in the non-adiabatic limit $(\Delta_k^2/\alpha_k << 1)$, $T_{LZ,k}$ is given as $T_{LZ,k} \sim 1/\sqrt{\alpha_k}$. It should be noted that for the linear quenching of the magnetic field $h(t) = t/\tau$, $\alpha_k = 1/\tau$.

Generalizing to the case of periodic quenching, $T_{LZ,k} \sim \Delta_k/(2\omega\sqrt{h_0^2 - J^2\cos^2 k})$, in the adiabatic limit while in the non-adiabatic limit, $T_{LZ,k} \sim 1/(\sqrt{2\omega\sqrt{h_0^2 - J^2\cos^2 k}})$. The transitions are localized around $t_{0,k}$ as compared to the time period for one cycle of the magnetic field if $T_{LZ,k}$ is less than the time period of one oscillation, i.e., $T_{LZ,k} << \pi/\omega$. This means that for $h_0^2 >> J^2$, in the adiabatic limit, $\Delta_k << h_0$, and in the non-adiabatic limit, $\omega << h_0$. This leads to the conclusion that the equation (10) describing the non-adiabatic transition probability is valid only for large h_0 and small ω. In the defect density for small ω (i.e. $\omega < \pi(J_x - J_y)^2/\sqrt{h_0^2 - J^2}$) only the modes close $k \sim 0, \pi$ contribute, resulting to a kink density at $t = 0$ given by

$$n \approx \frac{\sqrt{\omega\sqrt{h_0^2 - J^2}}}{\pi|J_x - J_y|} \qquad [\omega < \frac{\pi(J_x - J_y)^2}{\sqrt{h_0^2 - J^2}}] \tag{11}$$

The analytical results for p_k and hence the density of defects (obtained from Eq. 11) match exactly with the transition probabilities obtained by numerical integration of the Schrödinger Eqns for $h_0 >> \Delta_k, \omega$ as shown in Figs. 1 and 2. From Eq. 11, we find that in the limit $h_0 >> J$, the defect density shows a scaling form $n \sim (h_0\omega)^{1/2}$ which can be generalized using the Kibble-Zurek argument that assumes that the non-adiabatic transition is only dominant at a time when the characteristic time scale of the system is of the order of the rate of change of the Hamiltonian[6,7,9]. In the limit of large h_0 and small ω, we can generalize the above prescription to derive a

scaling form for the defect density for a single crossing the quantum critical point due to the periodic driving of the transverse field given by $n \sim (h_0\omega)^{\nu d/(\nu z+1)}$ where ν and z are the exponents associated with the quantum critical point and d is the spatial dimension of the system.

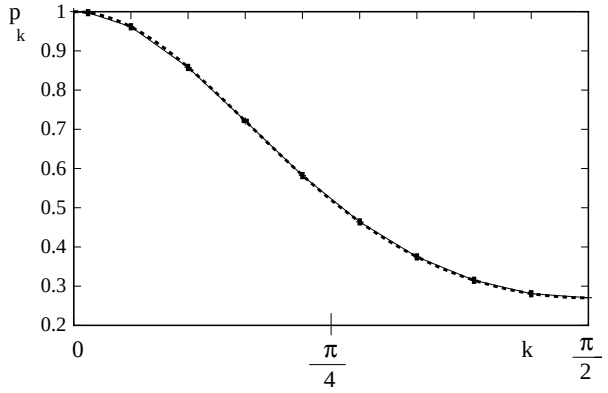

FIG. 1: p_k vs k as obtained numerically (solid line) and analytically (dashed line) for $h_0 = 20$, $\omega = 0.0003$, $|J_x - J_y| = 0.05$, and $J = 1$.

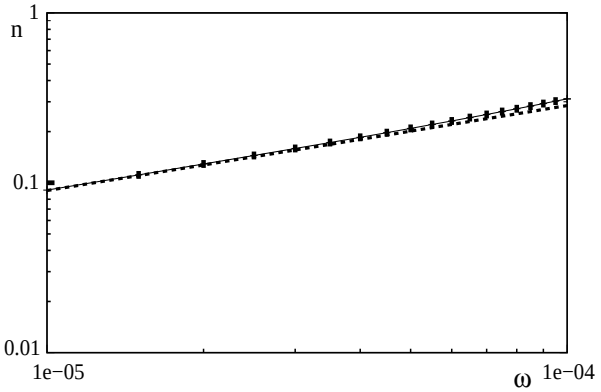

FIG. 2: n vs ω for $h_0 = 20$, $|J_x - J_y| = 0.05$ and $J = 1$. Solid line is found by numerically integrating p_k over k, and the dashed line is the plot of eqn. (11). Analytical and numerical results match exactly for lower values of ω.

A. Entropy

Following a recent paper by R. Barankov and A. polkovnikov[31], we define the diagonal entropy $s_d(k)$ for each k mode by

$$s_d(k) = -\sum_l \rho_{ll,k} ln \rho_{ll,k} \tag{12}$$

where $\rho_{ll,k} = \langle l|\rho_k|l\rangle$, ρ_k being the instantaneous density matrix of the system for the mode k. One advantage of using the diagonal entropy is that, it follows the thermodynamical relations as expected to be followed by entropy defined at higher temperatures. The diagonal entropy becomes identical to the previously defined Von Neumann entropy (s_{VN}), given by $s_{VN} = -\int_0^\pi tr(\rho_k ln \rho_k) dk/\pi$, when the off-diagonal terms in the density matrix, evaluated at the final time, go to zero upon coarse graining over k space[11,12,24]. We have checked the variation of the diagonal entropy density, evaluated at the final time, with ω by numerically integrating $s_d(k) = p_k ln p_k + (1-p_k) ln(1-p_k)$ over all k, with p_k obtained from eqn. (10). It is seen that the entropy attains a maximum near $\omega = \omega_0 = \pi(J_x - J_y)^2/h_0 ln2$ where the non-adiabatic transition probability (see Eq. 10) for the mode $k = \pi/2$ is half, and falls off on either side of ω_0. It should be noted that ω_0 closely resembles the characteristic time scale τ_0 appearing in the case of linear quenching[11].

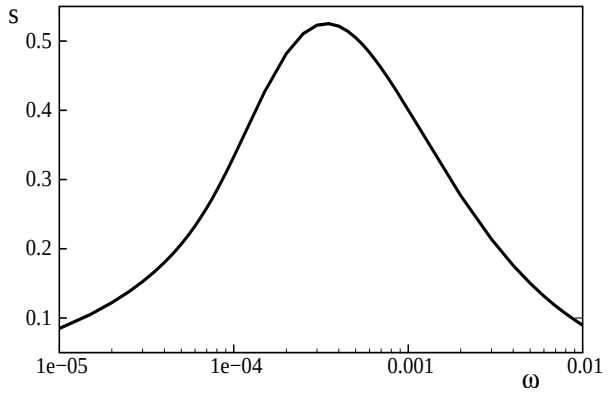

FIG. 3: Variation of diagonal entropy density with ω for one half cycle with $h_0 = 20, |J_x - J_y| = 0.05$ and $J = 1$, as obtained by numerical integration of $s_d(k)$ using the analytical expressions of p_k (eq. 10). The entropy for one half cycle attains maxima near $\omega \sim \omega_0 = \pi(J_x - J_y)^2/h_0 \ln 2$.

III. OSCILLATORY QUENCHING THROUGH A QUANTUM CRITICAL POINT: MULTIPLE CROSSINGS

Let us now focus on the repeated quenching case when the spin chain is periodically driven through the quantum critical point. In the present section, it will be shown that interference plays a major role in deciding the behaviour of the system, and for some choices of parameters, the phases will add up destructively to make the tunneling probability almost zero. In order to be able to treat the successive Landau Zener transitions , as independent events, the time between two successive crossings has to be greater than the Landau Zener transition time for a single crossing as mentioned in the previous section. To attain this limit we shall once again restrict our study to large values of h_0 and small ω. The system is prepared in the state $|1\rangle$ at time $t = 0$. The diagonal terms of the Hamiltonian for each modes k vanish, and consequently the gap becomes minimum, when the

magnetic field crosses the $-J\cos k$ line as shown in Fig. 4.

When the system approaches the crossing points of the diabatic levels, the energy gap is minimum leading to large relaxation time and the system fails to evolve adiabatically and the non-adiabatic transitions take place. 0n the other hand, away from the crossing points, the system follows adiabatic dynamics. Consequently, the evolution matrices associated with the system are different for close to and away from the crossing points[21,22]. Between the crossings, the system evolves following the

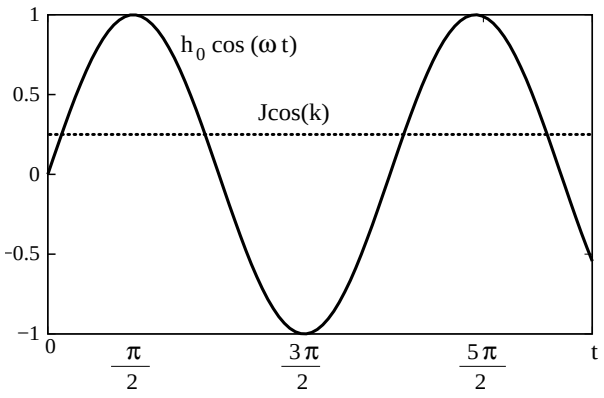

FIG. 4: Variation of energy levels due to the application of an oscillatory transverse field. The gap becomes minimum at the points where the magnetic field (shown by oscillatory solid line) becomes equal to $-J\cos k$.

matrix

$$G_j = \begin{bmatrix} e^{-i\theta_j} & 0 \\ 0 & e^{i\theta_j} \end{bmatrix},$$

where j denotes the direction in which the system goes through the crossing points. The LZ crossing in the non-adiabatic region can be approximately described by the evolution matrix

$$G_{LZ,j} = \begin{bmatrix} \cos\frac{\chi}{2} & \sin\frac{\chi}{2}e^{i\theta_{LZ,j}} \\ -\sin\frac{\chi}{2}e^{-i\theta_{LZ,j}} & \cos\frac{\chi}{2} \end{bmatrix},$$

where the angle χ is given by

$$\sin^2\frac{\chi}{2} = 1 - \exp(-2\pi\gamma) \tag{13}$$

where γ is defined in the previous section and j once again defines the direction of quenching (with respect to the crossing point). We have suppressed the notation k denoting the wave vector for the time being. Also

$$\theta_{LZ,1} \approx \frac{\pi}{2} + \theta_{stokes} \tag{14}$$

$$\theta_{LZ,2} \approx \frac{\pi}{2} - \theta_{stokes} \tag{15}$$

$$\theta_{stokes} = \frac{\pi}{4} + arg\Gamma(1-i\gamma) + \gamma(ln\gamma - 1) \tag{16}$$

where $\Gamma(x)$ is the gamma function and $\theta_{stokes} \to \pi/4$ or $\theta_{stokes} \to 0$, as $\gamma \to 0$ or $\gamma \to \infty$ respectively. If the system is repeatedly quenched with the sinusoidal field a series of Landau Zener crossings take place with the evolution of the system described by the successive application of matrices defined above. More specifically for one full cycle, i.e., ωt going from 0 to 2π, one can write the complete evolution matrix as a product of G_j and $G_{LZ,j}$, given by

$$G = G_{LZ,2}G_2G_{LZ,1}G_1, \tag{17}$$

which can be generalized for N complete cycles to the form

$$G_N = (G_{LZ,2}G_2G_{LZ,1}G_1)^N \ . \tag{18}$$

The probability amplitude of the states $|i\rangle$ $C_{i,N}$ $(i = 1, 2)$ at the final time $\omega t = 2N\pi$ therefore obeys the relation

$$\begin{bmatrix} C_{1,N} \\ C_{2,N} \end{bmatrix} = (G_{LZ,2}G_2G_{LZ,1}G_1)^N \begin{bmatrix} C_{1,0} \\ C_{2,0} \end{bmatrix} \tag{19}$$

where $C_{1,0} = 1$ and $C_{2,0} = 0$ at initial time $t = 0$. A little bit of algebra yields

$$G_{LZ,2}G_2G_{LZ,1}G_1 = \begin{bmatrix} g_{11} & g_{21} \\ -g_{21}^* & g_{11}^* \end{bmatrix} \tag{20}$$

where

$$\begin{aligned} g_{11} &= \cos^2\frac{\chi}{2}e^{-i(\theta_1+\theta_2)} - \sin^2\frac{\chi}{2}e^{i(-\theta_{LZ,1}+\theta_{LZ,2}-\theta_1+\theta_2)} \\ g_{21} &= \sin\frac{\chi}{2}\cos\frac{\chi}{2}(e^{i(\theta_{LZ,1}+\theta_1-\theta_2)} + e^{i(\theta_{LZ,2+\theta_1+\theta_2})}) \end{aligned} \tag{21}$$

Denoting the probability that for mode k the system is in state $|2\rangle$ after the nth crossing by $Q_{n,k}$, we get,

$$Q_{1,k} = (1 - p_k) \tag{22}$$

as seen in the previous section and for one complete full period of oscillation

$$Q_{2,k} = 4p_k(1-p_k)\sin^2(\theta_{stokes} + \theta_2) \tag{23}$$

For small anisotropy i.e., $(J_x - J_y)^2 << \omega\sqrt{h_0^2 - J^2\cos^2 k}$ we have $\theta_{stokes} \to \pi/4$, and θ_1 and θ_2 are given by

$$\begin{aligned} \theta_2 &= 2\int_0^{\pi/2\omega} \sqrt{(h_0\cos\omega t + J\cos k)^2 + \Delta_k^2} \\ &\approx (\frac{2h_0 + J\pi\cos k}{\omega}) \end{aligned} \tag{24}$$

$$\begin{aligned} \theta_1 &= 2\int_{\pi/2\omega}^{\pi} \sqrt{(h_0\cos\omega t + J\cos k)^2 + \Delta_k^2} \\ &\approx (\frac{-2h_0 + J\pi\cos k}{\omega}). \end{aligned} \tag{25}$$

Subsituting Eqs. 24 and 25 in Eq. 23, we get[19,20]

$$Q_{2,k} = 4p_k(1-p_k)\sin^2(\frac{2h_0 + J\pi\cos k}{\omega} + \frac{\pi}{4}). \tag{26}$$

$Q_{2,k}$ as obtained numerically and analytically as given in Eq. 26 are plotted as a function of k in fig. (5) and (6). The numerical plot is fairly in agreement with the analytical results. It is seen that $Q_{2,k}$ oscillates, with the tunneling probability going to zero for many k's, showing the signatures of constructive and destructive interferences.

It is clear that for very small ω, $Q_{2,k}$ oscillates rapidly with k due to the presence of the sinusoidal term in eq. (26). As a result the coarse grained or average $Q_{2,k}$ (denoted by $\overline{Q}_{2,k}$), obtained by integrating each $Q_{2,k}$ over a small range around that k followed by normalization, gives

$$\overline{Q}_{2,k} = 2p_k(1-p_k), \tag{27}$$

as obtained previously for repetition under linear quenching[24]. It has been shown in recent works[11,12,24] that, for linear quenching, we can evaluate the transition probabilities at the end of each cycle by using the coarse grained density matrix only, thereby simplifying the problem greatly by neglecting the off-diagonal terms in the matrix. Analogously, in the present case also, the characterstic time scale associated with the rate of change of the off-diagonal terms in the density matrix for a mode k sets the critical value of ω below which we can safely denote the tunneling probability by the coarse grained expression of Q_{2k} only, thereby yielding eq. (27)[19]. One concludes that in the limit of very small ω, the time interval between two successive crossings is large enough to destroy the phase information in the coarse grained probabilities.

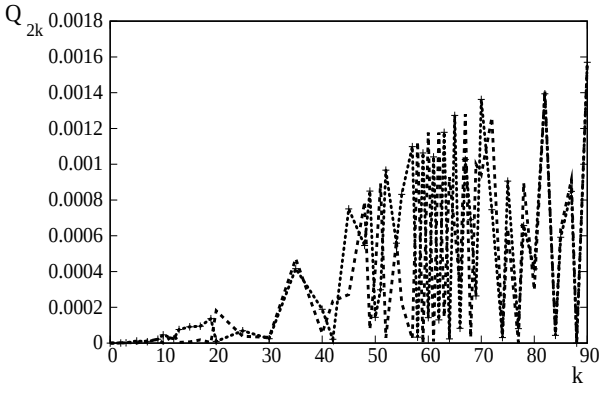

FIG. 5: Variation of $Q_{2,k}$ with k for $h_0 = 20, |J_x - J_y| = 0.005$, $\omega = 0.01$ and $J = 1$. The widely spaced dashed line is analytical, and the numerical data points are shown on the closely spaced dashed line.

To generalize to the case of many complete periods, it is useful to recast eqn. (20) in the form as[21]

$$G_{LZ,2}G_2G_{LZ,1}G_1 = \begin{pmatrix} \cos\frac{\zeta}{2} & \sin\frac{\zeta}{2}e^{i\phi} \\ -\sin\frac{\zeta}{2}e^{-i\phi} & \cos\frac{\zeta}{2} \end{pmatrix} \begin{pmatrix} e^{-i\theta/2} & 0 \\ 0 & e^{i\theta/2} \end{pmatrix} \tag{28}$$

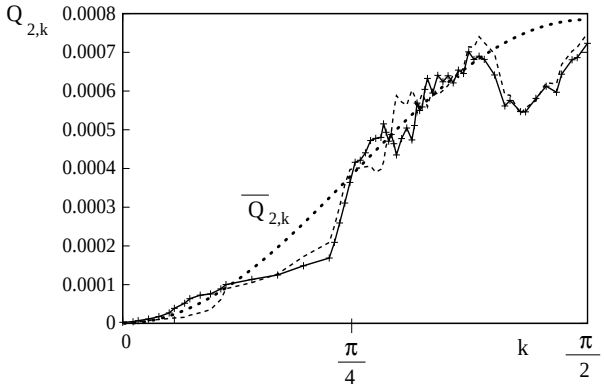

FIG. 6: Variation of $Q_{2,k}$ with k for $h_0 = 20, |J_x - J_y| = 0.005$, $\omega = 0.01$ and $J = 1$ obtained by averaging out the oscillations of the data shown in fig. 5. The dashed line is analytical, and the solid line is numerical. The smooth dotted line is the plot of course grained excitation probability $\overline{Q_{2,k}}$ as obtained from eq. (27).

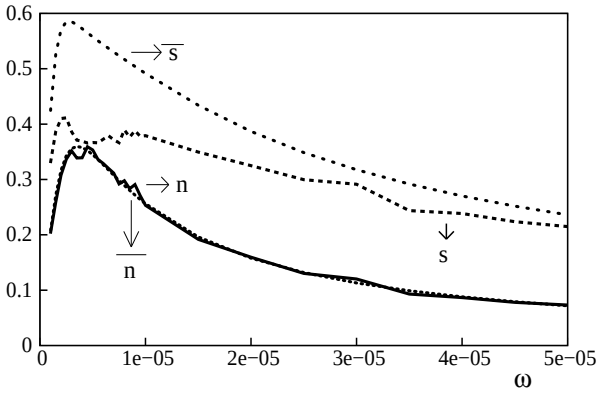

FIG. 7: Variation of actual and course grained kink density and entropy density with ω for $h_0 = 20, |J_x - J_y| = 0.005$ and $J = 1$ for one complete cycle, obtained by numerically integrating $Q_{2,k}$ and $\overline{Q_2k}$ in eq. (26) and eq. (27) respectively. The actual and course grained plots for kink density match reasonably well, whereas we see a significant difference in case of entropy density, eventhough their qualitative behaviours show similarity for a wide range of ω. The peaks of the plots occur near ω_0.

We shall call the diagonal matrix as U_1 and the other as U_2 which successively operate on the column matrix $(C_{1,k}, C_{2.k})$. The angles ζ and θ are given as

$$\sin^2\frac{\zeta}{2} \approx 4\sin^2\frac{\chi}{2}\cos^2(\frac{\theta_{LZ,1}-\theta_{LZ,2}}{2}-\theta_2) \tag{29}$$

$$\theta = \tan^{-1}\frac{A}{B} \tag{30}$$

where

$$A = \cos^2\frac{\chi}{2}\sin(\theta_1+\theta_2) + \sin^2\frac{\chi}{2}\sin(\theta_{LZ,1}-\theta_{LZ,2}+\theta_1-\theta_2)$$

and

$$B = \cos^2\frac{\chi}{2}\cos(\theta_1+\theta_2) - \sin^2\frac{\chi}{2}\cos(\theta_{LZ,1}-\theta_{LZ,2}+\theta_1-\theta_2)$$

$$\phi \approx \frac{\theta_{LZ,1}+\theta_{LZ,2}}{2} - \theta_2 \quad (31)$$

The dynamics described by Eq. (28) can be understood by exploring the properties of the rotation matrices U_1 and U_2. The role of U_2 is to rotate a vector about an axis in the $x-y$ plane by an angle of ζ, whereas the matrix U_1 brings about a rotation of the vector by an angle θ around the z axis only[32]. If θ is a multiple of 2π, which we call the resonance condition, the z-axis rotation does not affect the dynamics and the small oscillations of ζ add up constructively to produce full oscillations between the diabatic states $|1\rangle$ and $|2\rangle$. On the other hand, if θ differs from a multiple of 2π by more than ζ, then the rotations about angle ζ do not add up constructively, and the oscillations will be suppressed, thus resulting in an effective rotation about an axis almost parallel to the z axis only[21] (see figure 9). In the present context, the resonance condition is given by,

$$\theta \approx 2(\theta_1+\theta_2) = \frac{4\pi J\cos k}{\omega} = 2n\pi, \quad (32)$$

i.e.,

$$\frac{2J\cos k}{\omega} = n \quad (33)$$

Therefore for the resonance conditions, we can write

$$\begin{bmatrix} C_{1,N} \\ C_{2,N} \end{bmatrix} = \pm \begin{pmatrix} \cos\frac{\zeta}{2} & \sin\frac{\zeta}{2}e^{i\phi} \\ -\sin\frac{\zeta}{2}e^{-i\phi} & \cos\frac{\zeta}{2} \end{pmatrix}^N \begin{bmatrix} C_{1,0} \\ C_{2,0} \end{bmatrix}$$

From this formalism it is clearly seen that for the resonance conditions, after N complete cycles, we get N successive rotations by the small angle ζ. This causes oscillations in the probabilities of the two states with frequency given by

$$\Omega = \frac{\zeta}{2\pi/\omega} = \frac{\omega\zeta}{2\pi} = \frac{\omega}{\pi}\sin^{-1}[2\sqrt{1-p_k}\cos(\theta_{stokes} - \frac{2h_0+J\pi\cos k}{\omega})]. \quad (34)$$

Since ζ depends on the wave vector k, the probabilities for each resonant mode oscillates with its own characteristic frequency. As a result the kink density as well as the entropy density obtained by integrating over all modes shows an oscillatory behaviour (see figure 10). The oscillatory behaviour of the entropy density observed here is an artifact of retaining the phase information of the off-diagonal terms of the density matrix. It can be shown that in absence of phase information, $|C_{1,k}(\bar{t})|^2, |C_{2,k}(\bar{t})|^2 \to 1/2$ after each crossing, and as a result the entropy density of the system increases monotonically[24] with the number of crossings.

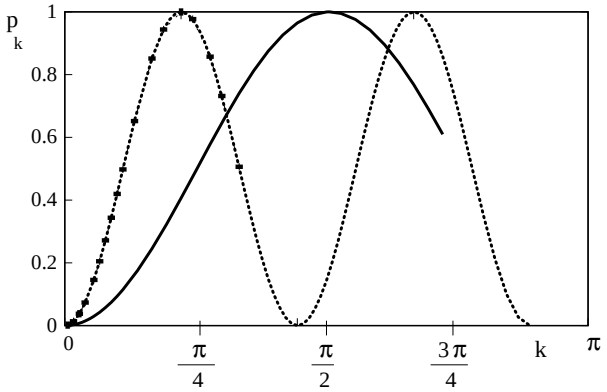

FIG. 8: Graph showing the behaviour of the excitation probability as a function of number of full cycles for $h_0 = 20, (J_x - J_y) = 0.005$, $J = 1$ and $\omega = 0.01$. The dashed line is obtained analytically for $k = 81.9521^0$ with integral $2J\cos k/\omega = 28$, while the solid line is the analytical graph for $k = 25.8419^0$ with integral $2J\cos k/\omega = 180$. Numerical data points shown on the dashed line corresponding to $k = 81.9521^0$ match exactly with the analytical results.

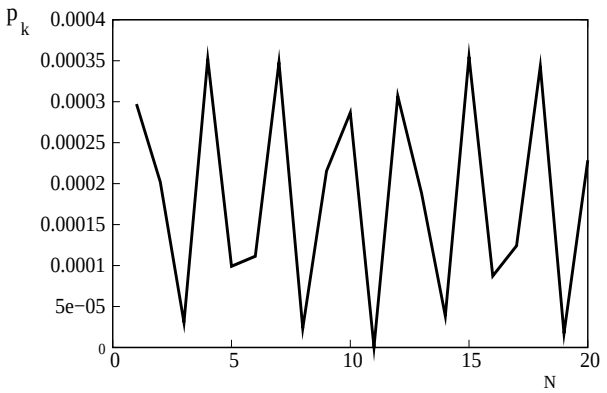

FIG. 9: Graph showing the behaviour of the excitation probability as a function of number of full cycles, obtained analytically for $h_0 = 20, |J_x - J_y| = 0.005$, $J = 1$, $\omega = 0.01, k = 80^0$ and non-integral $2J\cos k/\omega$. As expected, the excitation probability varies randomly and does not differ appreciably from its initial value.

IV. QUENCHING BY A MAGNETIC FIELD VARYING BOTH LINEARLY AND PERIODICALLY

In this section, we study the defect generation in a transverse XY spin chain driven by a time-dependent magnetic field $h(t)$ which consists of a linear part as well as an oscillatory part given by $h(t) = t/\tau + h_0\cos\omega t$ where τ denotes the rate of the linear part of the quenching. In the limit $h_0 \to 0$, the dynamics reduces to the well studied Kibble-Zurek problem of linear quenching while in the other limit of $\tau \to \infty$, one should recover the results presented in earlier sections. The presence of both the linear and periodic terms non-trivially modifies the density of defect in the final state as shown below. The

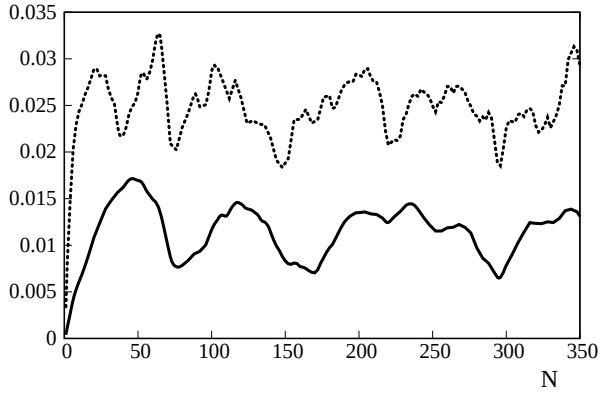

FIG. 10: Graph showing the behaviour of the kink density (solid line) and entropy density (dashed line) as a function of number of full cycles for $h_0 = 20, |J_x - J_y| = 0.005$, $J = 1$, and $\omega = 0.01$, as obtained by numerically integrating the excitation probabilities obtained by using eqn. (19).

reduced Hamiltonian in the present situation is given by

$$H_k(t) = \begin{bmatrix} \epsilon & i(J_x - J_y)\sin k \\ -i(J_x - J_y)\sin k & -\epsilon \end{bmatrix},$$

with $\epsilon = t/\tau + h_0 \cos\omega t + J\cos k$ and we shall once again recall the parametes α_k and Δ_k as defined before.

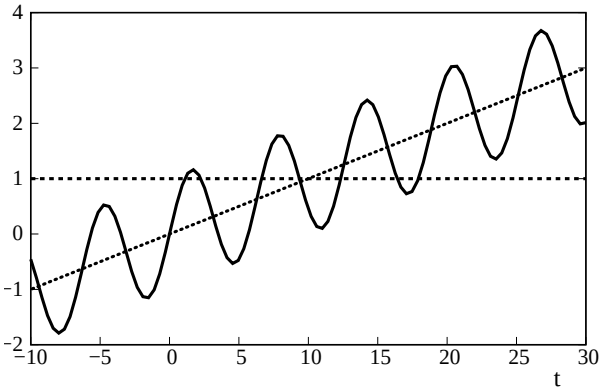

FIG. 11: Graph showing the behaviour of the diabatic energy levels with time when a linearly varying magnetic field is applied in addition to the oscillatory term. The inclined dotted line is the plot of $t/10$, the solid line is $\frac{t}{10} + \cos t$, and the dashed line parallel to x axis is the constant $-J\cos k = 1$.

For a given wavevector k, the instantaneous energy gap is minimum at times $t_{0,k}$ such that

$$\frac{t_{0,k}}{\tau} + h_0 \cos\omega t_{0,k} + J\cos k = 0 \tag{35}$$

Since $\cos\omega t_{0,k} \leq 1$ always, so from the above equation we can conclude that all the $t_{0,k}$'s occur in the time interval $-\tau(J + h_0) < t_{0,k} < \tau(J + h_0)$. Also, since time between two successive $t_{0,k}$'s is of the order of π/ω, so we can estimate the number of times that the gap goes to minimum for any k is $\sim \frac{2h_0\tau}{\pi/\omega}$, with the minimum number of times being 1. The situation is depicted in Fig. 11.

In the adiabatic limit ($\Delta_k^2/\alpha_k >> 1$) the Landau Zener transition time[29,33] (τ_{LZ}) is given as $\tau_{LZ} \sim \Delta_k^2/\alpha_k$, and in the non-adiabatic case, we have $\tau_{LZ} \sim 1/\sqrt{\alpha_k}$. It should be noted in the present case, the rate of change of diagonal terms $\alpha_k = |\frac{d}{dt}2(\frac{t}{\tau} + h_0\cos\omega t + J\cos k)|_{t_{0,k}} = 2|\frac{1}{\tau} - h_0\omega\sin\omega t_{0,k}|$. Hence for our theory to be valid, i.e., to get widely separated non-overlapping LZ transitions, we need $\tau << \frac{\pi}{\omega(J_x - J_y)}$ for the adiabatic and $\sqrt{\tau} << \frac{\pi}{\omega}$ for the non-adiabatic situations.

We prepare the system in its ground state at $t \to -\infty$ with $|C_{1,k}(-\infty)|^2 = 1$ and the probability of defect for the mode k in the final state at $t \to +\infty$ is given by the probability $|C_{1,k}(+\infty)|^2$. For the linear as well as periodic driving, Eq. 8 when linearized around the crossing point $t = t_{0,k}$ gets modified to

$$\begin{aligned} \frac{d^2C_{1,k}}{d^2t} &+ 2i((\frac{1}{\tau} - h_0\omega\sin\omega t_{0,k})(t - t_{0,k}))\frac{dC_{1,k}}{dt} \\ &+ \Delta_k^2 C_{1,k} = 0, \end{aligned} \tag{36}$$

which leads to the non-adiabatic transition probability

$$p_k = e^{-\frac{\pi\Delta_k^2}{\frac{1}{\tau} - h_0\omega\sin\omega t_{0,k}}} \tag{37}$$

In the limit of small τ and large ω, we can expand the excitation probability as $p_k \approx 1 - \frac{\pi(J_x - J_y)^2\sin^2 k}{1/\tau - h_0\omega\sin\omega t_{0,k}}$. Further, for $\frac{1}{\tau} >> h_0\omega\sin\omega t_{0,k}$, we can write the expression for kink density as

$$\begin{aligned} n &\approx \frac{1}{\pi}\int_0^\pi [1 - \frac{\pi(J_x - J_y)^2\sin^2 k}{1/\tau - h_0\omega\sin\omega t_{0,k}}]dk \\ &\approx 1 - \frac{\pi(J_x - J_y)^2}{2}\tau. \end{aligned} \tag{38}$$

The approximate equation given in Eq. (38) matches perfectly with the numerical integration results (see Fig. 13). On the other hand, in the limit of large τ and small ω, only the modes close to $k = 0$ or π contribute to the defect density, and by considering only the 0 and k modes in $t_{0,k}$, we can arrive at an approximate analytical expression given by

$$\begin{aligned} n = \frac{1}{\pi}\int_0^\pi p_k dk &= \frac{\pi\sqrt{\frac{1}{\tau} - h_0\omega\sin\omega t_{0,0}}}{2|J_x - J_y|} \\ &+ \frac{\pi\sqrt{\frac{1}{\tau} - h_0\omega\sin\omega t_{0,\pi}}}{2|J_x - J_y|} \end{aligned} \tag{39}$$

The kink density as a function of τ for the non-adiabatic and adiabatic cases, as obtained from equations (38) and (39) respectively, are plotted in Figs. 13 and 14 together with the corresponding numerically obtained values. As expected, in case of non-adiabatic evolution, we get exact matching between analytical and numerical results only for low values of τ for which $\frac{1}{\tau} >> h_0\omega\sin t_{0,k}$, whereas

in case of adiabatic evolution, we see good agreement between the analytical and numerical results only when $\frac{1}{\tau}$ is not close to $h_0 \sin\omega t_{0,0}$ or $h_0 \sin\omega t_{0,\pi}$, since around these values of τ, the effects of $h_0 \sin\omega t_{0,k}$ for $k \neq 0, \pi$ become important.

It should be noted that for the single crossing case, using the similar line of arguments given in section II, one can propose a generalized Kibble- Zurek scaling form of the defect density in the final state given as

$$n \sim a_0[|\frac{1}{\tau} - h_0\omega \sin\omega t_{0,0}|^{\nu d/(\nu z+1)}] + a_\pi[|\frac{1}{\tau} - h_0\omega \sin\omega t_{0,\pi}|^{\nu d/(\nu z+1)}], \quad (40)$$

where a_0 and a_π are two constants.

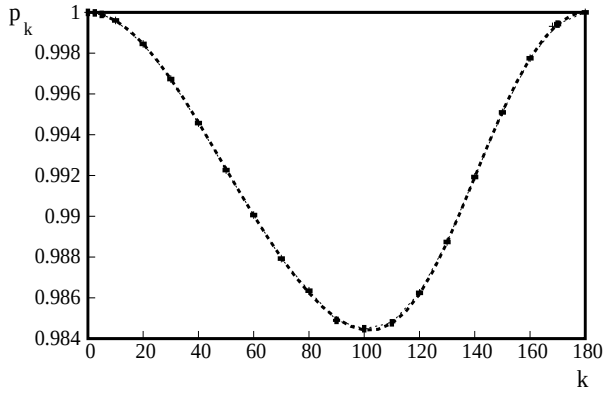

FIG. 12: p_k vs k (in degrees) for the case when gap becomes minimum only once, with $\tau = 2, h_0 = 1, \omega = 0.1, |J_x - J_y| = 0.05$ and $J = 10$. The dashed line is analytical and the numerical results shown as data points coinside exactly with the analytical values.

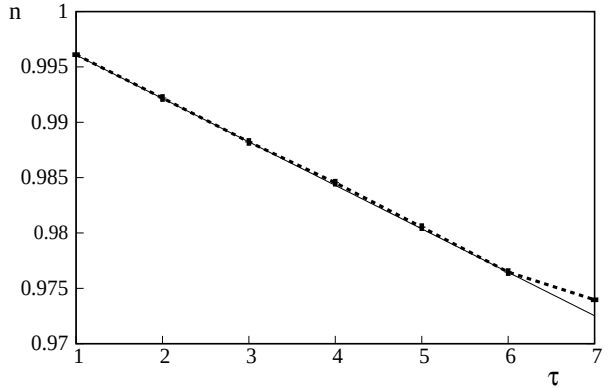

FIG. 13: Kink density (n) vs τ for $h_0 = 1, \omega = 0.1, |J_x - J_y| = 0.05$ and $J = 10$. The solid line is the plot of eq. (38), and the dashed line is obtained by numerical integration of the analytical expression of p_k as given in eq. (37). We get exact matching between the two results for low τ only, as expected from the theory. Only single crossing occurs for the range of τ shown in the figure.

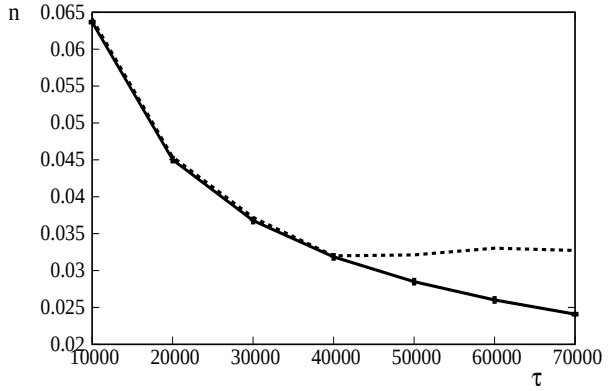

FIG. 14: Kink density n vs τ for $h_0 = 1, \omega = 0.000001, \Delta = 0.05$ and $J = 10$. Only single crossing occurs for the range of τ shown in the figure. The dashed line is found by numerical integration of eq. (37), and the solid line is obtained by using eq. (39). We get exact matching between the two results except when $\frac{1}{\tau}$ is very close to $h_0\omega \sin\omega t_{0,0}$ or $h_0\omega \sin\omega t_{0,\pi}$.

Now we concentrate on the situation of multiple crossings of the energy minima. For multiple crossings to occur for a given wave vector k, Fig. 11 implies that there should exist a $t = \bar{t}$ such that $\frac{1}{\tau} - h_0\omega \sin\omega\bar{t} = 0$, i.e., $\sin\omega\bar{t} = \frac{1}{\tau h_0\omega}$. This is possible only if $|\frac{1}{\tau h_0\omega}| \leq 1$. The Schrodinger equations for the probability amplitudes can be put in the form

$$\frac{dC_{1,k}}{dt} = \Delta_k e^{i(\frac{t^2}{\tau} + \frac{2h_0 \sin\omega t}{\omega} + 2Jt\cos k)} C_{2,k} \quad (41)$$

$$\frac{dC_{2,k}}{dt} = \Delta_k e^{i(\frac{t^2}{\tau} + \frac{2h_0 \sin\omega t}{\omega} + 2Jt\cos k)} C_{1,k} \quad (42)$$

Using the relation $e^{\pm iz\sin\omega t} = \sum_{r=-\infty}^{\infty} J_r(z) e^{\pm ir\omega t}$, where $J_r(z)$ is the Bessel function of first kind of order r, given by

$$J_r(\eta) = \Sigma_{m=0}^{\infty} \frac{(-1)^m}{m!\Gamma(m+r+1)} (\frac{\eta}{2})^{2m+1}, \quad (43)$$

we recast the equation to the form

$$\frac{dC_{1,k}}{dt} = \Delta_k \sum_{r=-\infty}^{\infty} J_r(\frac{2h_0}{\omega}) e^{i(\frac{t^2}{\tau} + 2Jt\cos k + r\omega t)} C_{2,k}. \quad (44)$$

The terms on the R.H.S. of eqn. (44) being rapidly varying in time, $\frac{dC_{1,k}}{dt}$ attains a non-negligible value only when the phase is stationary. Using

$$\frac{t^2}{\tau} + 2Jt\cos k + r\omega t = \frac{1}{\tau}(t + \frac{2J\tau\cos k + r\omega\tau}{2})^2 - \frac{(2J\tau\cos k + r\omega\tau)^2}{4\tau} \quad (45)$$

we find that $\frac{dC_{1,k}}{dt}$ is non-negligible only close to $t = -\frac{2J\tau\cos k + r\omega\tau}{2}$, with $r = 0, \pm1, \pm2, ...$ The above relation

implies the existence of an effective phase transition for each value of r. Choosing $r = l$ (say) and denoting $C_{i,k}$ by $C_{i,k,l}$ $(i = 1, 2)$, we get

$$\frac{dC_{1,l,k}}{dt} = \Delta_k J_l e^{-i\frac{(2J\tau\cos k + l\omega\tau)^2}{4\tau}} e^{i\frac{1}{\tau}[t+\frac{2J\tau\cos k + l\omega\tau}{2}]^2} C_{2,l,k} \quad (46)$$

Invoking upon the transformation to a new variable $s = t + l\omega\tau/2$, we get

$$\frac{dC_{1,l,k}}{ds} = \Delta_k J_l e^{-i\frac{l^2\omega^2\tau^2 + 4J\tau^2 l\omega\cos k}{4\tau}} e^{-iJ^2\tau\cos^2 k} e^{\frac{i}{\tau}(s+J\tau\cos k)^2} C_{2,l,k} \quad (47)$$

Let us compare with purely linearly quenching case ($h_0 = 0$), when the above equation gets modified to

$$\frac{dC_{1,l,k}}{ds} = \Delta_k e^{-iJ^2\tau\cos^2 k} e^{\frac{i}{\tau}(s+J\tau\cos k)^2} C_{2,l,k} \quad (48)$$

The role of periodic modulation on top of the linear quenching is to renormalize Δ_k to $\overline{\Delta_k}$ with $\overline{\Delta_k} = \Delta_k J_l e^{-i\frac{l^2\omega^2\tau^2 + 4J\tau^2 l\omega\cos k}{4\tau}}$. Note that $\overline{\Delta_k}$ also vanishes at the quantum critical point for the modes $k = 0$ and π.

The dividing of the probability amplitudes for a given wave vector to different l values by using the Bessel's function can be visualized in the following way: The two energy levels for the wave vector k are assumed to consist of a number of sublevels[23], with probability amplitudes of the lth level being denoted by $C_{1,l,k}$ and $C_{2,l.k}$. Each sublevel undergoes a level crossing only once through the course of dynamics, and for the lth transition for the mode k, the incoming state (given by $\overrightarrow{C_{l-1,k}}$) and the outgoing state (given by $\overrightarrow{C_{l,k}}$) are connected by the transfer matrix[23]

$$M_{l,k} = \begin{bmatrix} D_{l,k} & \beta_{l,k} e^{-i\frac{l^2\omega^2\tau^2 + 4J\tau^2 l\omega\cos k}{4\tau}} \\ -\beta^*_{l,k} e^{-i\frac{l^2\omega^2\tau^2 + 4J\tau^2 l\omega\cos k}{4\tau}} & D_{l,k} \end{bmatrix},$$

where $D_{l,k} = \sqrt{p_{l,k}}$ and $\beta_{l,k} = sgn J_l(\eta)\sqrt{1 - p_{l,k}} e^{-i\phi_{l,k}}$, in which $p_{l,k} = e^{-\pi\tau\Delta^2 (J_l(\eta))^2}$, $\eta = 2h_0/\omega$ and $\phi_{l,k}$ is the Stokes phase given by

$$\phi_{l,k} = \pi/4 + arg\Gamma(1 - i\delta_{l,k}) + \delta_{l,k}(ln\delta_{l,k} - 1) \quad (49)$$

where $\delta_{l,k} = \tau\Delta_k^2 (J_l(\eta))^2/2$, in terms of the gamma function $\Gamma(z)$.

It should be noted that $J_l(\eta) \to 0$ for large l, and $\Sigma_{l\to-\infty}^{\infty} J_l^2(\eta) = 1$. So the transition is confined to a finite region, and the infinite series of recursive relation for $l \to \infty$ converges to a finite value. In case of l for which $J_l(\eta) \approx 0$, $M_{l,k}$ gets reduced to an identity matrix. Hence taking $J_l(\eta) = 0\ \forall l > l_f$ we can write the state vector $\overrightarrow{C}_{l,k}$= $(C_{1,l,k}, C_{2,l,k})$ as

$$\overrightarrow{C_{l,k}} = M_{l,k}\overrightarrow{C}_{l-1,k} = M_{l,k}M_{l-1,k}...M_{0,k}...M_{-l_f+1,k}M_{-l_f,k}\overrightarrow{C}_{in,k} \quad (50)$$

where $\overrightarrow{C}_{in,k}$ denotes the initial condition. The probability of excitation at infinite time is given by $p_k(\infty) = |C_{1,k}(\infty)|^2$.

$$p_k(\infty) = |C_{1,k}(\infty)|^2 = |\begin{bmatrix} 1 & 0 \end{bmatrix} M_{l_f,k}M_{l_f-1,k}... M_{0,k}...M_{-l_f+1,k}M_{-l_f,k}\overrightarrow{C}_{in,k}|^2 \quad (51)$$

We are interested in evaluating the defect density in the final state in the limit of large τ and hence the off-diagonal terms in the matrix $M_{l,k}$ vanish upon coarse-graining, i.e., upon integration over all k. This approximation leads to the final result for the coarse grained non-adiabatic transition probability given by

$$|C_{1,l,k}|^2 = p_{l,k}|C_{1,l-1,k}|^2 + (1 - p_{l,k})|C_{2,l-1,k}|^2 \quad (52)$$

after neglecting the cross terms. The effects of the critical points are manifested by $\overline{\Delta_k}$ vanishing at $k = 0, \pi$ and those modes do not evolve from their initial state.

Comparison between kink density obtained by numerical integration of Schrödinger equation and by using the approximate analytical eqns. (51) and (52) for different τ has been shown in figure (15). We also plot the diagonal entropy density in figures. (16) and (17). Although, the defect density in the final state decays with increasing τ, the entropy density is found to increase and ultimately saturates as τ increases. This is in sharp contrast to the cases of linear quenching[12,24] where it attains a maxima at a characteristic scale $\tau = \tau_0$, and falls off on either side of τ_0. This behaviour can be explained in the following way: for very small τ the system fails to evolve appreciably and therefore remains very close to its initial ordered state at the final time. For larger values of τ, the probabilities change which introduces disorder in the final state leading to higher value of entropy density . For very large τ, the linear term becomes insignificant compared to the oscillatory term in the Hamiltonian. Consequently, only the oscillatory quenching term contributes to the dynamics of the system, keeping the entropy of the system constant for a fixed value of ω. It is to be noted that the interaction between the levels depend on the value of $J_l(2h_0/\omega)$ which saturates in the limit of large ω if h_0 is held fixed irrespective of the values of l and k. As a result, the kink density and also entropy density saturate in the limit of large ω, as shown in fig. (17)

V. CONCLUSION

In conclusion, we have studied the effects of interference in the quenching dynamics of a one-dimensional transverse XY spin chains in the presence of a time-dependent magnetic field $h(t) = h_0\cos\omega t$ or $h(t) = t/\tau + h_0\cos\omega t$. The system is initially prepared in its ground state and we estimate the defect density and entropy density in the final state following the quench using both approximate analytical and direct numerical integration techniques. In all the situations, the analytical

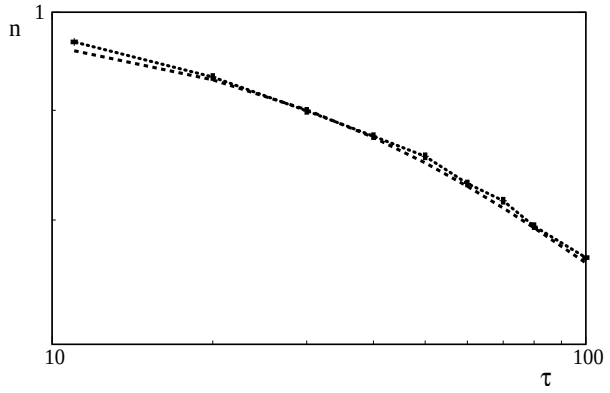

FIG. 15: Graph showing the variation of the kink density with τ for multiple crossings occurring with $h_0 = 1$, $(J_x - J_y) = 0.05$, $(J_x + J_y) = 10$, and $\omega = 0.1$. Results obtained by numerically solving Schrödinger equation (dotted line) match reasonably well with the analytical ones (dashed line).

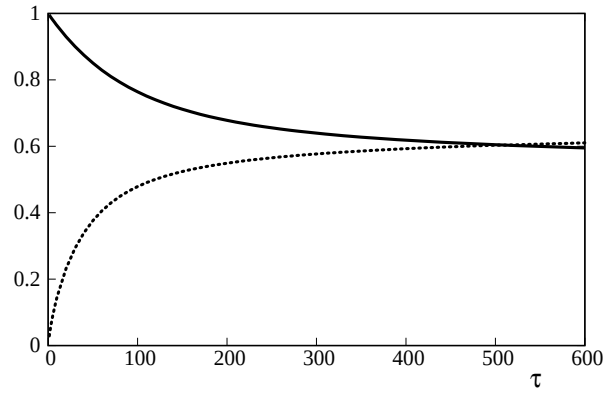

FIG. 16: Graph showing the variation of the kink density (solid line) and entropy density (dashed line) with τ as obtained analytically for $h_0 = 1$, $(J_x - J_y) = 0.05$, $(J_x + J_y) = 10$, and $\omega = 0.1$.

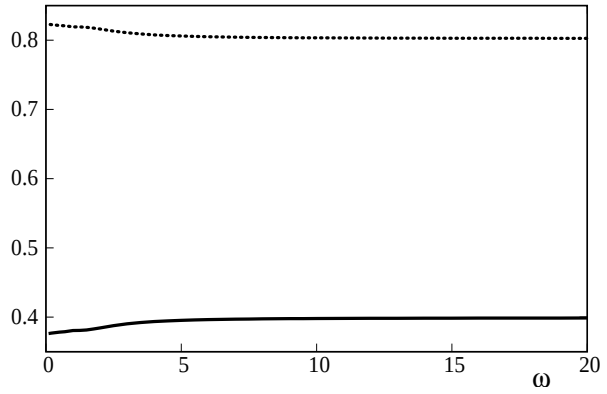

FIG. 17: Graph showing the variation of the kink density (solid line) and entropy density (dashed line) with ω as obtained analytically for $h_0 = 1$, $(J_x - J_y) = 0.05$, $(J_x + J_y) = 10$, and $\tau = 50$.

and numerical results are found to be in good agreement. Our observations presented in the paper are summarized as follows.

Firstly, we have studied the defect density in the final state following a single crossing by linearizing the oscillatory magnetic field round the time at which the instantaneous energy gap is minimmum. We show that in the limit of large h_0 and small ω, the defect density scales as $\sqrt{\omega}$. The observation is supported by numerical solution of the Schrodinger equation in the limit of small ω. On the other hand, the diagonal entropy density shows a maximum at a characteristic frequency scale ω_0 as defined in the text. Effects of interference are invisible in the case of a single crossing only. We do also suggest an equivalent Kibble-Zurek scaling relation for the defect density in the above situation.

In the next section we generalize to the multiple crossing situation where the interference of the probability densities play a dominant role. We use two different transfer matrices valid close to and away from the crossing points. We show that for a full cycle of oscillation the results obtained for repeated linear quenching[24] when the off-diagonal terms of the density matrix are coarse grained, leading to loss of phase information which gives rise to constructive and destructive interferences, is a valid approximation in the limit of small ω. For multiple crossings, we show that there exist resonance wave vectors for which the non-adiabatic transition probability oscillates between zero and one with the number of crossings following a characteristic k-dependent frequency. As a result the defect density also exhibits an oscillatory behaviour. The entropy density also shows a similar dependence on the number of crossings, which is in stark contrast with the linear quenching case, in which exclusion of the interference effects in the excitation probabilities causes the entropy density to increase monotonically with the number of crossings. It may be noted that a similar oscillatory behaviour is observed for the central spin of quantum Heisenberg chain[34].

Lastly, we study the quenching of the spin chain in the presence of a magnetic field which is varying linearly with time as t/τ and also modulated by a periodically varying part $h_0 \cos \omega t$. For the single crossing case, we once again use the linearization method which predicts a defect density that is in fair agreement with the numerically obtained result.For multiple crossings, we again invoke the transfer matrix approach to evaluate the cross-grained defect density. In this case it has been shown that for large values τ we can safely neglect the phase information, and hence the effects of interference, by coarse graining the density matrix. Our analytical and numerical results show that the defect density decreases with increasing τ for a given ω whereas when ω is varied with τ fixed, the defect density saturates for higher values of ω. The entropy density also exhibits a monotonic increase as a function of τ with fixed ω, an observation that is in sharp contrast with the linear quenching case where the entropy density attains a maximum at a char-

acteristic time scale τ_0[12] . This may be an artifact of the integrability of the model which gets decoupled into independent two-level systems[35].

Acknowledgements

AD acknowledges R. Moessener and the hospitality of MPIPKS, Dresden, where a major part of this work was done. We acknowledge Anatoli Polkovnikov, Diptiman Sen and Uma Divakaran for critical comments and helpful discussions.

* Electronic address: victor@iitk.ac.in
† Electronic address: dutta@iitk.ac.in

[1] S. Sachdev, *Quantum Phase Transitions* (Cambridge University Press, Cambridge, 1999).
[2] B. K. Chakrabarti, A. Dutta, and P. Sen, *Quantum Ising Phases and Transitions in Transverse Ising Models*, **m41** (Springer-Verlag, Berlin, 1996).
[3] I. Bloch, J. Dalibard, and W. Zwerger, Rev. Mod. Phys. **80**, 885 (2008); L. E. Sadler, J. M. Higbie, S. R. Leslie, M. Vengalattore and D. M. Stamper - Kurn, Nature (London) **443**, 312 (2006)
[4] T. Kadowaki and H. Nishimori, Phys. Rev. E **58**, 5355 (1998); K. Sengupta, S. Powell, and S. Sachdev, Phys. Rev. A **69**, 053616 (2004); P. Calabrese and J. Cardy, J. Stat. Mech: Theory Expt P04010 (2005), and Phys. Rev. Lett. **96**, 136801 (2006); A. Das, K. Sengupta, D. Sen, and B. K. Chakrabarti, Phys. Rev. B **74**, 144423 (2006); D. Rossini, A. Silva, G. Mussardo and G. Santoro, arXiv:0810.5508; S. Deng, G. Ortiz and L. Viola, arXiv:0809.2831, C. De Grandi, R. A. Barankov, and A. Polkovnikov, Phys. Rev. Lett, **101**, 230402 (2008), A. Polkovnikov and V. Gritsev, Nature Physics **4**, 477 (2008); S. Dorosz, T. Platini and D. Karevski, Phys. Rev. E **77**, 051120 (2008).
[5] R. Schützhold, M. Uhlmann, Y. Xu, and U. R. Fischer, Phys. Rev. Lett. **97**, 200601 (2006); C. Kollath, A. M. Läuchli, and E. Altman, Phys. Rev. Lett. **98**, 180601 (2007); S. R. Manmana, S. Wessel, R. M. Noack, and A. Muramatsu, Phys. Rev. Lett. **98**, 210405 (2007); M. Eckstein and M. Kollar, Phys. Rev. Lett. **100**, 120404 (2008); F. M. Cucchietti, B. Damski, J. Dziarmaga, and W. H. Zurek, Phys. Rev. A **75**, 023603 (2007);J. Dziarmaga, J. Meisner, and W. H. Zurek, Phys. Rev. Lett. **101**, 115701 (2008).
[6] T. W. B. Kibble, J. Phys. A **9**, 1387 (1976), Phys. Rep. **67**, 183 (1980).
[7] W. H. Zurek, Nature (London) **317**, 505 (1985), and Phys. Rep. **276**, 177 (1996).
[8] W. H. Zurek, U. Dorner, and P. Zoller, Phys. Rev. Lett. **95**, 105701 (2005).
[9] A. Polkovnikov, Phys. Rev. B **72**, 161201(R) (2005).
[10] J. Dziarmaga, Phys. Rev. Lett. **95**, 245701 (2005); B. Damski, Phys. Rev. Lett. **95**, 035701 (2005); B. Damski and W. H. Zurek, Phys. Rev. A **73**, 063405 (2006).
[11] R. W. Cherng and L. S. Levitov, Phys. Rev. A **73**, 043614 (2006).
[12] V. Mukherjee, U. Divakaran, A. Dutta, and D. Sen, Phys. Rev. B **76**, 174303 (2007).
[13] U. Divakaran and A. Dutta, J. Stat. Mech: Theory and Experiment P11001 (2007).
[14] D. Sen, K. Sengupta, and S. Mondal, Phys. Rev. Lett. **101**, 016806 (2008); R. Barankov and A. Polkovnikov, Phys. Rev. Lett. **101**, 076801 (2008).
[15] K. Sengupta, D. Sen, and S. Mondal, Phys. Rev. Lett. **100**, 077204 (2008); F. Pellegrini, S. Montangero, G. E. Santoro, and R. Fazio, Phys. Rev. B **77**, 140404(R) (2008);U. Divakaran, A. Dutta, and D. Sen, Phys. Rev. B 78, 144301 (2008).
[16] J. Dziarmaga, Phys. Rev. B **74**, 064416 (2006); T. Caneva, R. Fazio, and G. E. Santoro, Phys. Rev. B **76**, 144427 (2007).
[17] D. Patane, A. Silvia, L. Amico, R. Fazio, and G. Santoro, Phys. Rev. Lett. **101**, 175701 (2008).
[18] U. Divakaran, V. Mukherjee, A. Dutta, and D. Sen, J. Stat. Mech: Theory and Experiment P02007 (2009)).
[19] Y. Kayanuma, Phys. Rev. B, **47**, 9940 (1993).
[20] Y. Kayanuma, Phys. Rev. A, **50**, 843 (1994).
[21] S. Ashhab et. al., Phys. Rev. A, **75**, 063414 (2007).
[22] M. Wubs et. al., New Journal of Physics 7, 218 (2005).
[23] Y.kayanuma and Y.Mizumoto, Phys. Rev. A, **62**, 061401(R) (2000).
[24] V. Mukherjee, A. Dutta, and D. Sen, Phys. Rev. B **77**, 214427 (2008).
[25] E. Lieb, T. Schultz, and D. Mattis, Ann. Phys. (NY) **16**, 407 (1961); E. Barouch and B. M. McCoy, Phys. Rev. A **3**, 786 (1971).
[26] J. E. Bunder and R. H. McKenzie, Phys. Rev. B **60**, 344 (1999).
[27] C. Zener, Proc. Roy. Soc. London Ser A **137**, 696 (1932); L. D. Landau and E. M. Lifshitz, *Quantum Mechanics: Non-relativistic Theory*, 2nd ed. (Pergamon Press, Oxford, 1965).
[28] S. Suzuki and M. Okada, in *Quantum annealing and Related Optimization Methods*, edited by A. Das, and B.K. CHakrabarti (Springer-Verlag, Berlin 2005)
[29] N. V. Vitanov, Phys Rev. A, **59**, 988 (1999).
[30] N. V. Vitanov and B. M. Garraway, Phys. Rev. A, **53**, 4288 (1996).
[31] R. Barankov and A. Polkovnikov, arXiv:0806.2862v5 (2008).
[32] H. Goldstein, *Classical Mechanics*, Addison-Wesley (1990) see the chapter "The kinematics of rigid body motion".
[33] K. Mullen, E. Ben-Jacob, Y. Gefen, Z. Schuss, Phys. Rev. Lett, **62**, 2543 (1989).
[34] X.-Z. Yuan, K. -D. Zhu and H. -S. Goan, Eur. Phys. D **46**, 375 (2008).
[35] A. Polkovnikov, 2009 (private communications).